MSM-Based Integrated CMOS Wavelength-Tunable Optical Receiver

Ray Chen, *Student Member, IEEE*, Henry Chin, *Student Member, IEEE*, David A. B. Miller, *Fellow, IEEE*, Kai Ma, *Student Member, IEEE*, and James S. Harris, Jr., *Fellow, IEEE*

***Abstract*—We demonstrate a novel GaAs-metal–semiconductor–metal (MSM)-based wavelength-selective photodetector integrated with its complementary metal–oxide–semiconductor (CMOS) driver and receiver. This receiver has ∼1-ns wavelength switching access time and has been shown to detect 4 bits of 460-Mb/s (2.17-ns bit period) emulated data in nonreturn-to-zero format during the enabled 8.68-ns windows. The demonstrated channel spacing is ∼70.8 GHz. To our knowledge, this is the fastest reported wavelength switching time for a tunable optical receiver.**

***Index Terms*—Dense wavelength-division multiplexing, metal–semiconductor–metal (MSM) photodetector, optical access network, optical code-division multiple-access, reconfigurable wavelength-division multiplexing network, telecommunication, tunable filter, tunable optical receiver, tunable photodetector.**

I. Introduction

RAPID wavelength tuning is crucial for modern optical networks to achieve high bandwidth efficiency. Rapidly tunable lasers with a few tens of nanoseconds tuning times have been employed in optical network design [1] for dynamic wavelength allocation. The complementary component, rapidly tunable receivers, would provide further flexibility in network designs. Unfortunately, all of the currently available tunable filters or tunable receiver modules have relatively long wavelength-switching access times, ranging from a few seconds to a few microseconds depending on the device's working principle [2].

In our new approach [2], we interfere a beam with a delayed version of itself to form an interference pattern on top of the fingers of a metal–semiconductor–metal (MSM) photodetector. The fingers can be individually biased to different voltages. Then we can choose an appropriate MSM biasing pattern such that only the net photocurrent collected is from the desired wavelength, with cancellation of the current from the undesired wavelengths. Since the biasing pattern is simply a set of voltages, the wavelength reconfiguration speed is essentially limited only by the electronic switching times for the bias pattern. This detector can be scaled up for multiple wavelength discrimination by adding more interference patterns and MSM sections and more complex complementary metal–oxide–semiconductor (CMOS) control, as briefly discussed in Section V.

Manuscript received December 13, 2004; revised February 6, 2005. This work was supported by the Defense Advanced Research Projects Agency (DARPA) under the Chip-Scale WDM Program through ARO.

R. Chen, H. Chin, and D. A. B. Miller are with Solid State and Photonics Lab., Department of Electrical Engineering, Stanford University, Stanford, CA 94305 USA (e-mail: raychen@stanford.edu).

K. Ma and J. S. Harris, Jr. are with Center for Integrated System, Stanford University, Stanford, CA 94305 USA.

Digital Object Identifier 10.1109/LPT.2005.846579

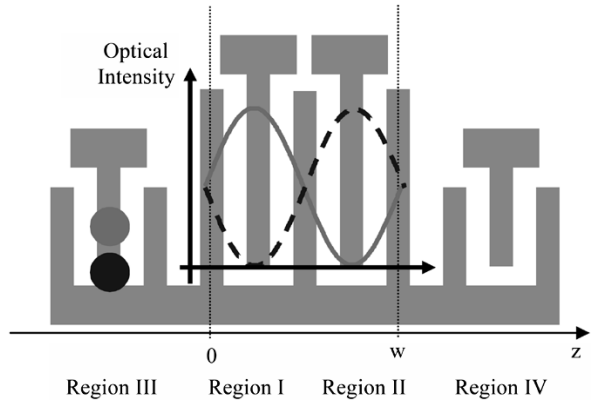

Fig. 1. Tunable MSM device, with the interference patterns of two wavelength channels λ_0 and $\lambda_0 + \Delta\lambda$ shown as solid and dashed lines. (Note: each interference pattern has a minimum of zero intensity.)

In this letter, we demonstrate an integrated wavelength tunable optical receiver, with the detector bonded to CMOS driver and receiver electronics, and show experimental results for wavelength switching under CMOS control with emulated nonreturn-to-zero (NRZ) data readout by the CMOS receiver.

II. Device Operation Principle

The key to wavelength selectivity in this device is to form a wavelength-dependent interference pattern that lines up with the MSM fingers in the center part of the device, and to bias the two top electrodes in Regions I and II of the device in Fig. 1 with equal magnitudes but opposite polarity to respond to specific interference patterns. Methods to set up such a wavelength-dependent interference pattern are given in [2] and [3], based on interfering a beam with a delayed version of itself at an appropriate angle between the beams. In our work, we use a Michelson Interferometer to generate two beams with an optical path length difference, and interfere them onto the detector with an angle between them. This angle dictates the interference pattern's spatial period, which should match the width of the switching part of the device w, as shown in Fig. 1. The optical path length difference between the two beams dictates the channel spacing $\Delta\lambda$.

Since the channel spacing $\Delta\lambda$ is much smaller than the central wavelength λ_0 in wavelength-division-multiplexing applications, the widths of the single fringes formed by the different wavelengths $\lambda_0 + \Delta\lambda$ and λ_0 are approximately the same. The interference pattern depends on wavelength, primarily through the spatial phase of the pattern. In particular, if the interference pattern is formed by interfering a beam with a delayed

version of itself, the spatial phase of the pattern (i.e., the position of the fringes) moves rapidly with wavelength; hence, the device can be a wavelength-sensitive photodetector. To make a detector that can respond to one of two different wavelengths, λ_0 or $\lambda_0 + \Delta\lambda$, while rejecting the other using the electrode pattern of Fig. 1, we shine the interfering signal beams on the detector, and also shine another controlled portion of the original signal beam (with no interference) on Region III. This additional beam on Region III is adjusted to obtain complete cancellation of the photocurrent from the rejected wavelength. The electrode in Region III is always positively biased, and hence, always contributes a positive net photocurrent. If we would like to enable the wavelength shown as the solid line interference pattern (formed by λ_0), while disabling the wavelength shown as the dashed line interference pattern (formed by $\lambda_0 + \Delta\lambda$), we positively bias the electrode in Region I and negatively bias the electrode in Region II. The positive photocurrent from the $\lambda_0 + \Delta\lambda$ portion of the beam on Region III cancels the net negative photocurrent that results from the dashed interference pattern (formed by $\lambda_0 + \Delta\lambda$), thereby canceling all the photocurrent for the signal beam at $\lambda_0 + \Delta\lambda$. If on the other hand we would like to enable the dashed interference pattern at $\lambda_0 + \Delta\lambda$ while disabling the solid interference pattern at λ_0, we can swap the biasing of Regions I and II (while leaving the biasing of Region III always positive), i.e., positively biasing Region II and negatively biasing Region I with now overall cancellation of the net photocurrent for the signal beam at λ_0. Therefore, by choosing the biasing pattern applied on electrodes in Regions I and II, we can select one wavelength while deactivating the other.

III. Device Structure and Integration With CMOS Electronics

The device in Fig. 2(a) is fabricated on a wafer with a 1-μm-thick undoped GaAs epitaxial active layer on a 0.3-μm $Al_{0.85}Ga_{0.15}As$ barrier layer on a semi-insulating GaAs substrate. The fabricated device in Fig. 2(a) consists of fingers in three regions, left, center, and right. The center part, which performs the wavelength switching, comprises two interdigitated sets of three biasing electrodes and one comb-like current summing electrode. All three parts have 1-μm finger width and spacing. The center part covers a 40 by 25 μm area. Each of the left and right side parts cover a 20 by 13 μm area. These side areas are used to adjust the overall spectral response dc level to achieve a good ON–OFF contrast ratio.

The fabricated device in Fig. 2(a) is designed for being flip-chip bonded onto the CMOS controller and readout chip. The whole detector and electrode region is formed on a mesa, with the active epilayer being removed everywhere else. The area between the wavelength switching part of the device and the contrast ratio adjusting (side) parts of the device is etched with two square holes as markers for accurate interference pattern alignment. Indium bumps are deposited on top of the device control nodes for flip-chip bonding to pads on the CMOS chip. Fig. 2(b) shows the CMOS driver, the flip-chip bonded wavelength selective photodetector after chemical removal of its substrate and its CMOS receiver in a single chip.

The CMOS driver is implemented by two inverter chains sized with equal delay but with one of the differential outputs

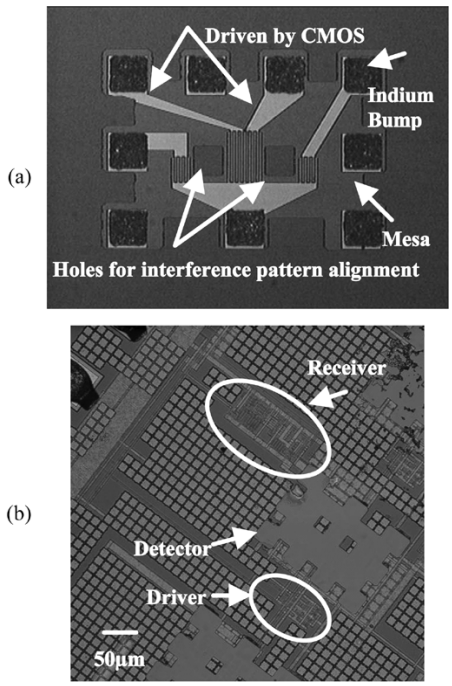

Fig. 2. (a) Fabricated MSM-based wavelength-selective photodetector for integration with its CMOS driver and receiver. (b) CMOS driver, the detector, and CMOS receiver in the same chip. The detector is seen from the bottom side, after chemical removal of the GaAs substrate.

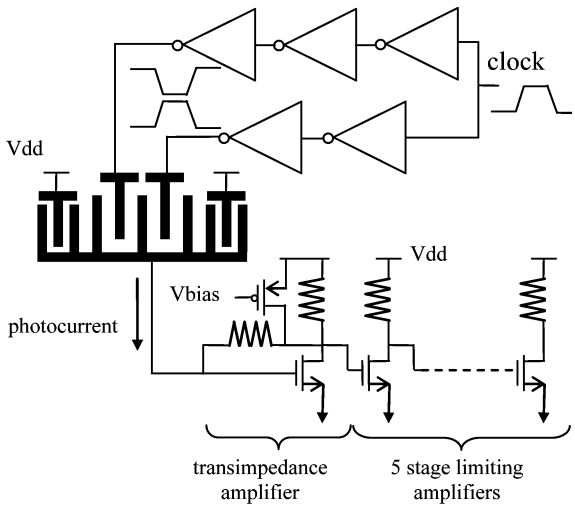

Fig. 3. Schematic drawing of the CMOS tunable optical receiver and its detector driver.

inverted with respect to the other, as shown in Fig. 3. The receiver consists of a single-ended transimpedance amplifier cascaded with five single-ended limiting amplifiers to drive the output pads of the chip. The photocurrent common node [i.e., essentially the bottom common electrode in Fig. 1, or the bottom center connection in Fig. 2(a)], is connected to the input node of the transimpedance amplifier, and is biased to half (1.25 V) of the supply voltage $V_{\rm dd}$ (2.5 V in this 0.25-μm CMOS technology). As a given MSM finger is biased either above or below this midpoint, the sign of its photocurrent contribution changes correspondingly because of the symmetric current–voltage behavior of MSMs [2].

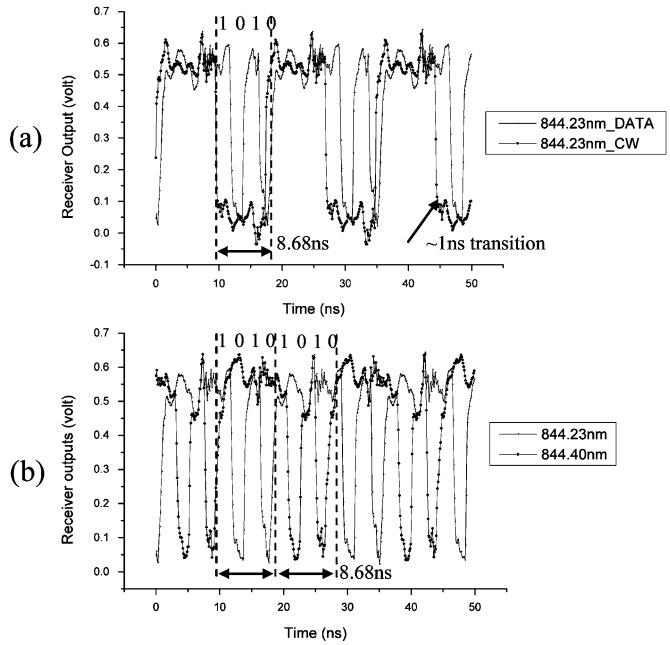

Fig. 4. Measured output waveforms from the CMOS receiver with flip-chip bonded tunable photodetector.

IV. Results and Discussion

To demonstrate the rapid wavelength switching ability of this photodetector along with its optical receiver, every 8.68 ns we alternate between two different biasing patterns on the MSM fingers using the CMOS driver circuit, and we look at the receiver's electrical output (Fig. 4). First we use an input wavelength of 844.23 nm [Fig. 4(a)]. We show results for two different optical inputs, one from a continuous-wave (CW) beam and the second from a DATA beam where we are turning the optical beam ON and OFF at ~230 MHz (synchronous with the 8.68-ns biasing pattern time) to emulate a simple 460-Mb/s data bit stream in NRZ format. (Note in these results that a negative-going signal results from a net photocurrent.) In Fig. 4(a), the 844.23nm_DATA trace shows that the receiver is enabling and disabling reception of the data on the carrier wavelength 844.23 nm every 8.68 ns. During the 8.68 ns when 844.23 nm is enabled, the receiver detects four emulated data bits in NRZ format with 2.17-ns bit period each (460 Mb/s). The other trace, 844.23nm_CW, shows that the receiver is enabling and disabling the 844.23-nm carrier wavelength with no data modulation every 8.68 ns. From the transition time of this CW trace, the wavelength switching access time is seen to be ~1 ns. In Fig. 4(b), the receiver alternately enables either 844.23 or 844.40 nm with an emulated 460-Mb/s NRZ data stream in both cases. Experimentally, the interference pattern with the 844.23-nm beam is aligned with the photodetector to get one trace. Then we temperature tune the Fabry–Pérot semiconductor laser source to a second wavelength, 844.40 nm, for the second trace. In Fig. 4(b), data modulated on 844.23 and 844.40 nm is enabled alternately. The measured photocurrent sensitivity of the optical receiver is ~60 μA for these output voltages, and the channel spacing is ~70.8 GHz.

V. Scalability of the Detector

This device architecture can be extended to discriminate more than two wavelengths. In general, discriminating N wavelengths would require at least $\log_2 N$ interference patterns and exactly N electrodes per pattern. The photocurrent generated by each pattern is summed by simply connecting the common nodes together. More refined shaping of the spectral response of the detector can be accomplished through more interference patterns and electrodes, to satisfy the desired specification for a particular application.

In the experimental results presented here, a biasing pattern on Regions I and II results in a photocurrent generated by the interference pattern that is sinusoidal with wavelength. To allow for the discrimination of four colors for example, we would add another MSM structure and illuminate it with a second interference pattern. However, this second pattern would have an optical path length difference between its beam pair such that the photocurrent would still be sinusoidal with respect to wavelength, but at twice the frequency compared to the first. In other words, the spectral response would be the second harmonic of the first pattern's response.

The addition of more interference patterns simply adds more harmonics, which can be weighted through the choice of biasing patterns and summed by collecting the photocurrent at a common node. This yields a set of orthogonal Fourier basis functions, and well-established Fourier processing techniques can be applied to the specific selection of needed interference patterns and electrode biasing patterns.

The control of these possibly numerous bias patterns at high switching speeds is readily achievable through integration of the photodetector with CMOS electronics. Hence, our demonstration of a fast two-color-discriminating photodetector shows the high promise of realizing future receivers capable of discriminating more wavelengths.

VI. Summary

A novel MSM-based integrated CMOS wavelength tunable optical receiver with ~1-ns wavelength switching access time is demonstrated. This low-voltage-biasing high-scalability tunable photodetector has a good compatibility with mainstream CMOS electronics controller for sophisticated biasing control with nanosecond scale wavelength switching access time.

Acknowledgment

The authors would like to acknowledge National Semiconductor for fabrication of the CMOS electronics.

References

[1] I. M. White, M. S. Rogge, K. Shrikhande, and L. G. Kazovsky, "A summary of the HORNET project: A next-generation metropolitan area network," *IEEE J. Sel. Areas Commun.*, vol. 21, no. 9, pp. 1478–1494, Nov. 2003.

[2] R. Chen, D. A. B. Miller, K. Ma, and J. S. Harris Jr., "Novel electrically controlled rapidly wavelength selective photodetection using MSMs," *IEEE J. Sel. Topics Quantum Electron.*, vol. 11, no. 1, pp. 184–189, Jan./Feb. 2005.

[3] D. A. B. Miller, "Laser tuners and wavelength-sensitive detectors based on absorbers in standing waves," *IEEE J. Quantum Electron.*, vol. 30, no. 3, pp. 732–749, Mar. 1994.